Analysis of the triplet production by the circularly polarized photon at high energies

G. I. Gakh, M. I. Konchatnij, I. S. Levandovsky, and N. P. Merenkov*

Kharkov Institute of Physics and Technology

61108, Akademicheskaya, 1, Kharkov, Ukraine

The possibility in principle of the determining high energy photon circular polarization by the measurement of the created electron polarization in the process of triplet photoproduction $\gamma + e^- \to e^+e^- + e^-$ is investigated. The respective event number which depend on polarization states of photon and created electron does not decrease with the growth of the photon energy, and this circumstance can ensure the high efficiency in such kind of experiments. We study different double and single distributions of the created electron (or positron), which allow to probe the photon circular polarization and to measure its magnitude (the Stock's parameter ξ_2), using the technique of the Sudakov's variables. Some experimental setups with different rules for event selection are studied and corresponding numerical estimations are presented.

1. INTRODUCTION

It is well known that process of the triplet production

$$\gamma(k) + e^-(p) \to e^-(k_1) + e^+(k_2) + e^-(p_1) \tag{1}$$

by the high-energy photons on the atomic electrons can be used to measure the photon linear polarization degree [1–3]. This possibility arises due to azimuthal asymmetry of the corresponding cross-section, i.e., due to its dependence on the angle between the plane in which the photon is polarized, and the plane $(\mathbf{k}, \mathbf{p}_1)$ where the recoil electron 3-momentum lies. The detailed description of the different differential distributions, such as the dependence on the momentum value, on the polar angle and minimal recorded momentum of the

* Electronic address: merenkov@kipt.kharkov.ua

recoil electron, dependence on the invariant mass of the created electron-positron pair, on the positron energy and others, has been investigated in Ref. [4]. This single-spin effect is the basis for theoretical background of polarimeters where the different angular and energy distributions are used [5].

The exact expressions for differential and partly integrated cross sections of the process (1) is very cumbersome and exist in the complete form only for unpolarized case [6]. At high collision energy only two (from eight) diagrams contribute with leading accuracy (neglecting terms of the order of m^2/s, $s = 2(kp)$, m is the electron mass) and the corresponding expressions are essentially simplified. These diagrams (the so-called Borselino diagrams [7]) are shown in Fig.1. Nevertheless, at the boundaries of the final particle phase space the non-leading terms can be reinforced, and in Ref. [8] some of such effects had been investigated for the case of linearly polarized photons.

As regards the photon circular polarization, it can be probed by at least double-spin effects. In the region of small and intermediate photon energies the circular polarization can be measured using double-spin correlation in the Compton scattering. For example, in Ref. [9] the corresponding possibility was considered for the Compton cross-section asymmetry in the scattering of photon on polarized electrons. In principle, one can also measure the polarization of the recoil electron. The double-spin effects may be used to create polarized electron beams using the laser photons [10].

At high energies of the photon beams the use of the Compton scattering is not effective because the Compton cross-section decreases very fast with the growth of the photon energy. If the photon energy is large, the cross-section of the electron-positron pair production, which does not decrease with the growth of the energy, has become larger than the Compton scattering one. To estimate the respective energy one can use the asymptotic formulas for the total cross-sections [11]

$$\sigma_C \approx \frac{2\pi r_0^2}{x}\ln x\,, \quad \sigma_{pair} \approx \frac{28\alpha r_0^2}{9}\ln x\,, \tag{2}$$

$$x = \frac{s}{m^2}\,,\ \alpha = \frac{1}{137}\,,$$

where $r_0 = \alpha/m$ is the classical radius of electron. In the rest system of the initial electron ($s = 2\omega m$) the photon energy ω has to be larger than for about $80\,MeV$. Thus, to measure the circular polarization of the photons with the energies more than $100\,MeV$ it is advantageously to use the process (1) rather than the Compton scattering.

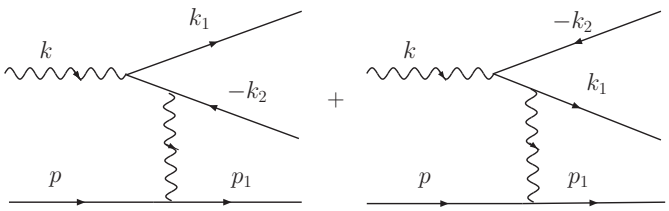

Fig.1. *Borselino diagrams which give the nondecreasing contribution in the cross section at high energies and small momentum transferred.*

The above estimate of the pair production cross-section is made taking into account only the Borselino diagrams. The events, described by these diagrams, have very specific kinematics in the rest system of the initial electron, namely: the recoil electron has small 3-momentum (of the order of m) whereas the created electron-positron pair carries out all the photon energy and moves along the photon momentum direction. In the reaction c.m.s the scattered (recoil) electron has small (of the order of m) perpendicular momentum transfer and very small (of the order of m^3/s) longitudinal one. Just such kind of the events contribute to the nondecreasing cross-section. The contribution of the rest diagrams, describing the direct capture of the photon by the initial electron and exchange effects due to the identity of the final electrons, decreases at least as m/ω.

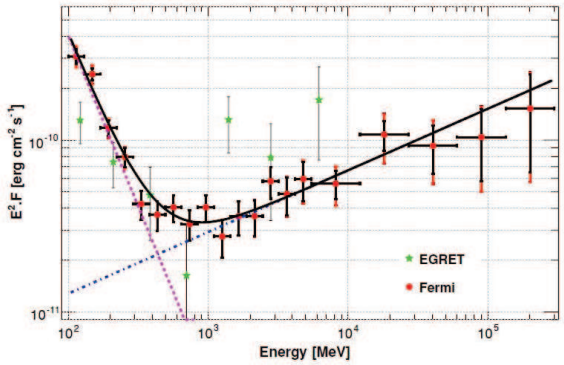

Fig.2. *Spectral energy distribution of the Crab Nebula renormalized to the total phase interval. The synchrotron radiation (region up to* $10^3\,MeV$*) and due to inverse Compton scattering (region upper* $10^3\,MeV$*) are presented. To clarify the experimental points, statistical and systematic errors, solid and dotted curves see Refs. [12, 13].*

The very high-energy photon component can be contained in the cosmic rays. For exam-

ple, in Fig. 2 we show the spectral energy distribution of the Crab Nebula [12]. In this figure the high-energy photons in the region of $10^2 - 10^3 MeV$ are synchrotron ones and in the region $10^3 - 10^5 MeV$ they arise due to possibility of the inverse Compton scattering on an ultra-energetic electrons. The analysis of their polarization is very important to understand the remarkable features of the cosmologically distant gamma ray bursts.

There are a few possibilities to measure the photon circular polarization in the process (1). It is possible: i) to use longitudinally polarized electrons and measure the asymmetry of the cross-section at two opposite directions of the polarization, ii) to measure the polarization of the recoil electrons, iii) to measure the polarization of the created electrons or positrons. The double-spin correlation effects in first two cases decrease with the growth of the photon energy and, therefore, are not effective for the measurement of the photon circular polarization at the high energies. So, in this paper we concentrate on the third experimental setup which can be realized in the scattering of the photons on unpolarized atomic electrons or the electron beam. Our study in some aspects is close to the approach developed in Ref. [14], where the process (1) with circularly polarized photons has been suggested to create high energy polarized electrons, and in the last section we discuss the corresponding similarities and differences in more details.

2. FOUR-RANK COMPTON TENSOR

In the approximation considered here, the matrix element squared of the process (1) is defined by a contraction of two second-rank Lorentz tensors $V_{\mu\nu}$ and $B_{\mu\nu}$, and the differential cross-section of this process can be written in the form

$$d\sigma = \frac{e^6}{2(2\pi)^5 sq^4} V_{\mu\nu} B_{\mu\nu} d\Phi \,, \tag{3}$$

$$d\Phi = \frac{d^3k_1}{2E_1}\frac{d^3k_2}{2E_2}\frac{d^3p_1}{2\varepsilon_1}\delta(k+p-p_1-k_1-k_2) \,,$$

where $q = k - k_1 - k_2 = p_1 - p$, $E_1\,(E_2)$ is the energy of the created electron (positron) and ε_1 is the energy of the recoil electron with 4-momentum p_1. The tensor $B_{\mu\nu}$ is defined by the electron current j_μ

$$B_{\mu\nu} = j_\mu j_\nu^* \,, \quad j_\mu = \bar{u}(p_1)\gamma_\mu u(p) \,, \tag{4}$$

and in the case of polarized initial electron

$$B_{\mu\nu} = \frac{1}{2} Tr(\hat{p}_1 + m)\gamma_\mu(\hat{p} + m)(1 - \gamma_5 \hat{W})\gamma_\nu \,,$$

where W_μ is its polarization 4-vector. Taking the trace over the spinor indices we have

$$B_{\mu\nu} = q^2 g_{\mu\nu} + 2(pp_1)_{\mu\nu} - 2im(\mu\nu qW)\,, \tag{5}$$

where the following notation is used

$$(ab)_{\mu\nu} = a_\mu b_\nu + a_\nu b_\mu\,, \quad (\mu\nu qW) = \epsilon_{\mu\nu\lambda\rho} q_\lambda W_\rho\,, \quad \epsilon_{1230} = 1\,.$$

If the initial electron is unpolarized and one want to measure the recoil electron polarization, it needs to substitute

$$p \leftrightarrows p_1,\ \mu \leftrightarrows \nu,\ W \to W_1$$

in the right hand side of Eq. (5) which results simply to change $W \to W_1$, where W_1 is the polarization 4-vector of the recoil electron.

For events with arbitrarily polarized photon beam, the tensor $V_{\mu\nu}$ in Eq. (3) can be written in terms of its Stock's parameters ξ_i $(i = 1\,, 2\,, 3)$ and the four-rank Compton tensor $T_{\mu\nu\lambda\rho}$ (such that its contractions with $q_\mu\,, q_\nu$ and $k_\lambda\,, k_\rho$ equal to zero and which will be defined below) as follows

$$\begin{aligned} V_{\mu\nu} = \frac{1}{2}\big([e_{1\lambda}e_{1\rho} + e_{2\lambda}e_{2\rho}] + \xi_3[e_{1\lambda}e_{1\rho} - e_{2\lambda}e_{2\rho}] + \\ \xi_1[e_{1\lambda}e_{2\rho} + e_{2\lambda}e_{1\rho}] - i\xi_2[e_{1\lambda}e_{2\rho} - e_{2\lambda}e_{1\rho}]\big)T_{\mu\nu\lambda\rho}\,, \end{aligned} \tag{6}$$

where the mutually orthogonal space-like 4-vectors e_1 and e_2, relative to which the photon polarization properties are defined, have to satisfy the following relations

$$e_1^2 = e_2^2 = -1\,,\ (e_1 k) = (e_2 k) = (e_1 e_2) = 0\,.$$

The first term inside the parentheses in r.h.s. of Eq. (6) is in charge of the events with unpolarized photon, the second and third ones are responsible for the events with linear photon polarization and the last one – for the events with the circular polarization. The parameters ξ_1 and ξ_3, which define the linear polarization degree of the photon, depend on the choice of the 4-vectors e_1 and e_2, whereas parameter ξ_2 does not depend. Because we want to investigate the events with circular photon polarization, we can choose these 4-vectors by the most convenient way, namely

$$e_{1\lambda} = \frac{\chi_1 k_{2\lambda} - \chi_2 k_{1\lambda}}{N}\,, \quad e_{2\lambda} = \frac{(\lambda\, k\, k_1\, k_2)}{N} \tag{7}$$

with the short notation

$$N = 2\chi\chi_1\chi_2 - m^2(\chi_1^2 + \chi_2^2)\,,\ \chi_{1,2} = (kk_{1,2})\,,\ \chi = (k_1k_2)\,.$$

The 4-vector e_1 appears kindly in the expression for the four-rank Compton tensor $T_{\mu\nu\lambda\rho}$, see Eq.(8) below.

The polarization properties of a real photon are defined by two orthogonal 3-vectors $\mathbf{n_1}$ and $\mathbf{n_2}$. Each of these two vectors are orthogonal also to 3-vector of the photon momentum $\mathbf{k}$, and the 4-vectors e_1 and e_2 are their covariant generalizations. It follows from the definition of e_1 and e_2 that they have both time and space components. Adding to them 4-vector k with appropriate factors (it is, in fact, the gauge transformation), one can eliminate the time and longitudinal (along the vector $\mathbf{k}$) components. Thus, in arbitrary Lorentz system with Z-axis directed along the vector $\mathbf{k}$ and 3-momentum lying in the (ZX) plane, where

$$k = (\omega, 0, 0, \omega)\,,\ k_1 = (E_1, k_{1x}, 0, k_{1z})\,,\ k_2 = (E_2, k_{2x}, k_{2y}, k_{2z})\,,$$

the corresponding transformation has the form

$$(0, \mathbf{n_1}) = e_{1\lambda} - \frac{E_1k_{2z} - E_2k_{1z}}{N}\,k_\lambda\,,\ (0, \mathbf{n_2}) = e_{1\lambda} - \frac{k_{1x}k_{2y}}{N}\,k_\lambda,$$

where

$$\mathbf{n_1} = (n_x\,, n_y\,, 0)\,,\ \mathbf{n_2} = (n_y\,, -n_x\,, 0)\,,$$
$$n_x = \frac{\omega[(E_1 - k_{1z})k_{2x} - (E_2 - k_{2z})k_{1x}]}{N}\,,\ n_y = \frac{\omega(E_1 - k_{1z})k_{2y}}{N}\,,$$
$$N^2 = \omega^2\big\{[(E_1 - k_{1z})k_{2x} - (E_2 - k_{2z})k_{1x}]^2 + (E_1 - k_{1z})^2k_{2y}^2\big\}\,.$$

At such transformation no observables are changed due to the gauge invariance, that manifests itself by means of the above mention restrictions on the tensor $T_{\mu\nu\lambda\rho}$

$$k_\lambda T_{\mu\nu\lambda\rho} = k_\rho T_{\mu\nu\lambda\rho} = 0\,.$$

That is why the description of all polarization phenomena in process (1) by means of the 4-vectors e_1 and e_2 is completely equivalent to the description in terms of 3-vectors $\mathbf{n_1}$ and $\mathbf{n_2}$. The evident advantage of the covariant description is independence from the Lorentz system.

For events in which the created electron polarization states in the process (1) must be determined, the Borselino diagrams lead to following expression for the tensor $T_{\mu\nu\lambda\rho}$

$$T_{\mu\nu\lambda\rho} = \frac{1}{2} Tr\big\{(\hat{k_1} + m)(1 - \gamma_5 \hat{S})\hat{Q}_{\lambda\mu}(\hat{k_2} - m)\hat{Q}_{\nu\rho}\big\}\,, \tag{8}$$

$$\hat{Q}_{\lambda\mu} = \frac{N}{\chi_1\chi_2} e_{1\lambda}\gamma_\mu + \frac{\gamma_\lambda \hat{k}\gamma_\mu}{2\chi_1} - \frac{\gamma_\mu \hat{k}\gamma_\lambda}{2\chi_2}\,,$$

where S is the electron spin 4-vector, with properties $S^2 = -1\,,\ (Sk_1) = 0\,.$

Let us divide $T_{\mu\nu\lambda\rho}$ into two parts: the firs part depends on 4-vector S and the second one does not

$$T_{\mu\nu\lambda\rho} = T^{(0)}_{\mu\nu\lambda\rho} + T^{(S)}_{\mu\nu\lambda\rho}\,.$$

Then we can write

$$T^{(0)}_{\mu\nu\lambda\rho} = T_{(\mu\nu)(\lambda\rho)} + T_{[\mu\nu][\lambda\rho]}\,, \tag{9}$$

$$T^{(S)}_{\mu\nu\lambda\rho} = im\big[T_{(\mu\nu)[\lambda\rho]} + T_{[\mu\nu](\lambda\rho)}\big]\,,$$

where we use the index notation $(\alpha\beta)$ $([\alpha\beta])$ to emphasize the symmetry (antisymmetry) under permutation of indices α and β. These symmetry properties (9) and form (5) for the tensor $B_{\mu\nu}$ allow to discuss some features of the process (1) with high energy polarized photon on the quality level.

As we noted in the Introduction, the cross section of the process (1) (when all particles are unpolarized) does not decrease with the growth of the photon energy. Such behavior is caused by the terms proportional to s^2 in the contraction $T_{\mu\nu\lambda\rho}B_{\mu\nu}$ which enters differential cross section (3). On the other hand, only symmetrical component $2(pp_1)_{\mu\nu}$ in Eq. (5) can ensure appearance of these terms. This simple observation suggest us that the non decreasing spin correlations in the differential cross section in considered case are connected only with symmetrical, relative $(\mu \leftrightarrows \nu)$ permutation, tensors $T_{(\mu\nu)(\lambda\rho)}$ and $T_{(\mu\nu)[\lambda\rho]}$. The first one describes single-spin correlations which depend on Stock's parameters ξ_1 and ξ_3 caused by the photon linear polarization [1]. The second one can contribute on condition that the polarization of the created electron (or positron) is measured, or in other words, it describes double-spin correlation which depends on Stock's parameter ξ_2 that is the degree of the photon circular polarization. In further we will concentrate just on this double-spin correlation that can be used to measure parameter ξ_2.

The antisymmetric, under $(\mu \leftrightarrows \nu)$ permutation, tensors $T_{[\mu\nu][\lambda\rho]}$ and $T_{[\mu\nu](\lambda\rho)}$ have not a large physical sense in the considered problem because they can describe the spin correlations

in the differential cross section which decrease with the energy growth at least as s^{-1}. For the full description in the such approximation there is not enough to consider only the Borselino diagrams and one have to account for all the rest six ones. But these tensors are connected by the cross symmetry with the corresponding tensors in annihilation channel which are suitable for description of the subprocess $e^+ + e^- \to \gamma + \gamma^*$, which is important in different radiative return measurements [15] and where there are no contribution of any other diagrams. That is why we give here all the corresponding expressions in very compact form

$$
\begin{aligned}
T_{(\mu\nu)(\lambda\rho)} = \frac{2}{\chi_1\chi_2}\Big\{ g_{\mu\nu}\Big[\big(\chi_1+\chi_2\big)^2 g_{\lambda\rho} - \frac{N^2}{\chi_1\chi_2}\, q^2\, e_{1\lambda}e_{1\rho}\Big] - \\
2\chi_1\chi_2(1+\hat{P_{\lambda\rho}})\, g_{\mu\rho}g_{\nu\lambda} - 2(k_1k_2)_{\lambda\rho}k_\mu k_\nu + \\
\big(1+\hat{P_{\lambda\rho}}+\hat{P_{\mu\nu}}+\hat{P_{\lambda\rho}}\hat{P_{\mu\nu}}\big)g_{\nu\rho}\big[k_\mu(\chi_2 k_{1\lambda}+\chi_1 k_{2\lambda}) + N(k_{1\mu}-k_{2\mu})e_{1\lambda}\big] + \\
N\Big[\frac{(k_1e_1)_{\lambda\rho}(kk_2)_{\mu\nu}}{\chi_1} - \frac{(k_2e_1)_{\lambda\rho}(kk_1)_{\mu\nu}}{\chi_1}\Big] - \\
g_{\lambda\rho}\big[(\chi_1+\chi_2)(k_{12}k)_{\mu\nu} - 2(m^2+\chi)k_\mu k_\nu\big]\Big\},
\end{aligned}
\tag{10}
$$

where $k_{12} = k_1 + k_2$ and $\hat{P_{\alpha\beta}}$ is operator of the $(\alpha \rightleftarrows \beta)$ permutation.

$$
\begin{aligned}
T_{[\mu\nu][\lambda\rho]} = \frac{2}{\chi_1\chi_2}\Big\{(1-\hat{P_{\mu\nu}})\Big[(\chi_1^2+\chi_2^2)g_{\mu\lambda}g_{\nu\rho} + \frac{(\chi_1^2k_{2\mu}-\chi_2^2k_{1\mu})k_\nu[k_1k_2]_{\lambda\rho}}{\chi_1\chi_2}\Big] + \\
(1-\hat{P_{\mu\nu}}-\hat{P_{\lambda\rho}}+\hat{P_{\mu\nu}}\hat{P_{\lambda\rho}})\Big[\frac{N}{\chi_1\chi_2}g_{\nu\lambda}e_{1\rho}(\chi_2^2k_{1\mu}-\chi_1^2k_{2\mu}) + \\
\frac{\chi_1^2-(\chi_1-\chi_2)(m^2+\chi)}{\chi_1}g_{\mu\rho}k_\nu k_{1\lambda} + \frac{\chi_2^2-(\chi_2-\chi_1)(m^2+\chi)}{\chi_2}g_{\mu\rho}k_\nu k_{2\lambda}\Big]\Big\},
\end{aligned}
\tag{11}
$$

where we use notation $[ab]_{\alpha\beta} = a_\alpha b_\beta - a_\beta b_\alpha$.

The spin-dependent parts of $T_{\mu\nu\lambda\rho}$ read

$$
\begin{aligned}
T_{[\mu\nu](\lambda\rho)} = -2(\mu\nu qS)h_\lambda h_\rho + \frac{(\mu\nu qk)}{\chi_1^2\chi_2}\big[(\chi_2-\chi_1)(kS)g_{\lambda\rho} - \\
\chi_1\chi_2(Sh)_{\lambda\rho}\big] - \frac{(kS)}{\chi_1}\big[h_\lambda(\mu\nu\rho q) + h_\rho(\mu\nu\lambda q)\big],
\end{aligned}
\tag{12}
$$

where 4-vector h is defined as

$$
h = \frac{k_2}{\chi_2} - \frac{k_1}{\chi_1},
$$

and

$$
T_{(\mu\nu)[\lambda\rho]} = \Big[\frac{(k_1k_1)_{\mu\nu}+(k_2k_2)_{\mu\nu}}{\chi_1\chi_2} - \Big(\frac{1}{\chi_1^2}+\frac{1}{\chi_2^2}\Big)(k_1k_2)_{\mu\nu} +
$$

$$+\frac{q^2(\chi_1-\chi_2)^2+\chi_1(\chi_1^2-\chi_2^2)}{2\chi_1^2\chi_2^2}\Big](\lambda\rho kS)+$$
$$+\frac{(\lambda\rho kk_{12})}{\chi_2}\Big[(Sh)_{\mu\nu}+(Sk_2)\Big(\frac{1}{\chi_1}-\frac{1}{\chi_2}\Big)g_{\mu\nu}\Big]+$$
$$\Big\{(\mu\lambda\rho k)\Big[\Big(\frac{(k_2S)}{\chi_2}-\frac{(kS)}{\chi_1}\Big)\Big(\frac{k_{2\nu}}{\chi_1}-\frac{k_{1\nu}}{\chi_2}\Big)+$$
$$\frac{(\chi_1-\chi_2)}{2\chi_1\chi_2^2}(q^2+2\chi_1+2\chi_2)S_\nu\Big]+(\mu\leftrightarrows\nu)\Big\}. \tag{13}$$

3. DIFFERENTIAL CROSS SECTION

When calculating the non-decreasing (with the energy growth) contribution to the unpolarized part of the cross section one ought to account for the terms proportional to s^2 in the contraction $T_{\mu\nu\lambda\rho}(e_{1\lambda}e_{1\rho}+e_{2\lambda}e_{2\rho})B_{\mu\nu}$, which arise due to scalar products (k_1p), (k_2p), and (kp). To do this it is enough to use approximation $B_{\mu\nu}=4p_\mu p_\nu$ (see Ref. [3]). Then we have

$$T_{\mu\nu\lambda\rho}(e_{1\lambda}e_{1\rho}+e_{2\lambda}e_{2\rho})B_{\mu\nu}=-16\Big[\frac{4m^2}{\chi_1\chi_2}(k_1p)(k_2p)+$$
$$(k_1p)^2\Big(\frac{q^2}{\chi_1\chi_2}-\frac{2m^2}{\chi_2^2}\Big)+(k_2p)^2\Big(\frac{q^2}{\chi_1\chi_2}-\frac{2m^2}{\chi_1^2}\Big)\Big]\,. \tag{14}$$

The main contribution to the differential cross section, within the chosen accuracy, gives the region of small momentum transferred $|q^2|\sim m^2$. In this case it is useful to introduce the so-called Sudakov's variables [16] which are suitable for the calculation at high energies and small momentum transferred. These variables, in fact, define the expansion of the final state 4-momenta on the longitudinal and transversal components relative to the 4-momenta of the initial particles. For the process (1) we have (see also [14])

$$k_2=\alpha p^{'}+\beta k+k_\perp\,,\ q=\alpha_q p^{'}+\beta_q k+q_\perp\,,$$
$$p^{'}=p-\frac{m^2}{s}k\,,\ s=2(kp)\,,\ p^{'2}=0\,,$$
$$(k_\perp p)=(k_\perp k)=(q_\perp p)=(q_\perp k)=0\,,$$
$$d^4k_2=\frac{s}{2}d\alpha d\beta d^2k_\perp\,,\ d^4q=\frac{s}{2}d\alpha_q d\beta_q d^2q_\perp\,, \tag{15}$$

where the 4-vectors $k_\perp$ and $q_\perp$ are the space-like ones, so $k_\perp^2=-\mathbf{k}^2\,,\ q_\perp=-\mathbf{q}^2$, and $\mathbf{k}\,,\mathbf{q}$ are two-dimensional Euclidean vectors.

The phase space of the final particles with the over-all $\delta-$ function (see Eq. (3)) can be written as

$$d\Phi = \frac{s^2}{4} d\alpha d\beta d^2k_\perp d\alpha_q d\beta_q d^2q_\perp \delta(k_2^2 - m^2)\delta(k_1^2 - m^2)\delta(p_1^2 - m^2)\,. \tag{16}$$

By using the conservation laws we derive

$$k_2^2 = s\alpha\beta - \mathbf{k}^2\,,\ k_1^2 = -s(1-\beta)(\alpha+\alpha_q) - (\mathbf{k}+\mathbf{q})^2\,,$$

$$p_1^2 = s\beta_q + m^2 - \mathbf{q}^2\,,\ s\alpha = \frac{m^2+\mathbf{k}^2}{\beta}\,,\ s\beta_q = \mathbf{q}^2\,,$$

$$s\alpha_q = -\frac{m^2+\mathbf{k}^2}{\beta} - \frac{m^2+(\mathbf{k}+\mathbf{q})^2}{1-\beta}\,,$$

and after integration over $\alpha\,, \alpha_q\,, \beta_q$ by help of three δ-functions the phase space reduces to very simple expression

$$d\Phi = \frac{1}{4s\beta(1-\beta)} d\beta d^2\mathbf{k} d^2\mathbf{q}\,, \tag{17}$$

The variable β is the photon energy fraction that is carried out by the positron $\beta = E_2/\omega$ (the created electron energy $E_1 = (1-\beta)\omega$). In terms of the Sudakov's variables, the independent invariants are expressed as follows

$$\chi_1 = \frac{m^2+(\mathbf{k}+\mathbf{q})^2}{2(1-\beta)},\ \chi_2 = \frac{m^2+\mathbf{k}^2}{2\beta},\ q^2 = -\mathbf{q}^2 - \frac{m^2(m^2+\mathbf{k}^2)^2}{s^2\beta^2(1-\beta)^2}. \tag{18}$$

Further we will consider two possible experimental situations: i) when both the scattered (recoil) and created electron are recorded, ii) only created electron is recorded. In the first case we suggest that events with $|q^2| < |q_0^2|$ are not detected, where the minimal selected momentum transfer squared $|q_0^2|$ is of the order of m^2. In the second case all events with $|q^2| \geq |q_{min}^2|$ are included, where $|q_{min}^2|$ is the minimal possible value of $|q^2|$, which is defined by the second term in the expression for $-q^2$ in Eq. (18). It is just the longitudinal momentum transfer squared.

These two event selections give very different values for the differential cross section. If $|q^2|$ is of the order of m^2 one can neglect everywhere with q_{min}^2. Such procedure leads to the cross section that depends on q_0, but does not depend on the collision energy (invariant s). On the other hand, when values of $|q^2|$ for selected events begin from q_{min}^2, the integration over $d^2\mathbf{q}$ leads to logarithmic rise of the corresponding cross section when the collision energy increases. This leading logarithmic contribution can be derived by the equivalent photon method [17] but our goal is to calculate also the next-to-leading (constant) one.

We begin with consideration of the first experimental setup. Using the definition of the differential cross section (Eq. (3)) and relation (14), taking into account the phase space factor (17), expressions for independent invariants (18) and that in considered case

$$2(k_1p) = (1-\beta)s\,,\ 2(k_2p) = \beta s\,,\ q^2 = -\mathbf{q}^2,$$

we obtain

$$d\sigma = \frac{2\alpha^3}{\pi^2\mathbf{q}^4}\Big[2m^2\beta(1-\beta)\Big(\frac{1}{m^2+(\mathbf{k}+\mathbf{q})^2} - \frac{1}{m^2+\mathbf{k}^2}\Big)^2 + \frac{\mathbf{q}^2[1-2\beta(1-\beta)]}{[m^2+(\mathbf{k}+\mathbf{q})^2][m^2+\mathbf{k}^2]}\Big]d\beta d^2\mathbf{k}d^2\mathbf{q}\ . \tag{19}$$

Our goal is to derive distribution on the electron (positron) energy β and the perpendicular momentum transfer squared ($\mathbf{q}^2$). Thus, we have to integrate the r.h.s. of Eq. (19) over $d^2\mathbf{k}$, and the effective values of $|\mathbf{k}|$ of the order of m. Because integral rapidly converges we can take 0 and ∞ as the limits of integration over $|\mathbf{k}|$. After corresponding integration the differential cross section reads

$$\frac{d\sigma^l}{d\beta d\mathbf{q}^2} = \frac{4\alpha^3}{\mathbf{q}^4}\Big\{\big[1-2\beta(1-\beta)\big]\Psi_1 + 2\beta(1-\beta)\Psi_2\Big\}\ ,$$

$$\Psi_1 = \frac{1}{x}\ln\frac{x+1}{x-1},\quad \Psi_2 = 1-\frac{2m^2}{\mathbf{q}^2}\Psi_1, \tag{20}$$

$$x = \sqrt{1+\frac{4m^2}{\mathbf{q}^2}}\ .$$

In the limited case $\mathbf{q}^2/m^2 \gg 1\,, \Psi_1 = \ln(\mathbf{q}^2/m^2)\,, \Psi_2 = 1$. If contrary $\mathbf{q}^2/m^2 \ll 1$, the expression in the braces in r.h.s. of Eq. (20) has to be proportional to $\mathbf{q}^2$ due to the gauge invariance. In this case

$$\Psi_1 = \frac{\mathbf{q}^2}{2m^2}\Big(1-\frac{\mathbf{q}^2}{6m^2}\Big)\,,\ \Psi_2 = \frac{\mathbf{q}^2}{6m^2}.$$

Elementary integration this cross section over the positron energy fraction β

$$\frac{d\sigma^l}{d\mathbf{q}^2} = \frac{4\alpha^3}{3\mathbf{q}^4}\Big[1+2\Big(1-\frac{m^2}{\mathbf{q}^2}\Big)\Psi_1\Big]\,, \tag{21}$$

allows to find distribution over the recoil momentum l in the rest frame of the initial electron (formula (16) in Ref. [18]) which is connected with $\mathbf{q}^2$ by relation

$$\mathbf{q}^2 + 2m^2 = 2m\sqrt{m^2+l^2}.$$

This is a checking test of our calculation. But further we could not integrate over β because we have to leave the trace from the created pair.

For the pair creation in the process (1) by the high-energy photon on the relativistic initial electron with the energy $E \gg m$ at back-to-back collision, the scattered (recoil) electron can be detected, in principle, by means of the circular detector which sums all events with $\theta_{min} < \theta < \theta_{max}$, where the scattering electron angle $\theta = |\mathbf{q}|/E$. Here we bear in mind that the scattered electron energy ε_1 practically does not distinguish from the initial electron one E. In such experimental setup the differential cross-section (20) ought to be integrated over the detector aperture. The maximum and minimum values of $\mathbf{q}^2$ are defined by the angular dimensions of the detector.

$$\mathbf{q}^2_{min} = E^2\theta^2_{min}\ , \quad \mathbf{q}^2_{max} = E^2\theta^2_{max}\ .$$

For analytical integration it is convenient to introduce new variable $\mathbf{q}^2/m^2 = 4\sinh^2 z\,$, so that

$$\Psi_1 = 2z\tanh z,\ \ \Psi_2 = 1 - \frac{z}{\sinh z\cosh z},\ \ \frac{d\mathbf{q}^2}{\mathbf{q}^4} = \frac{\cosh z dz}{2m^2\sinh^3 z}\ .$$

and the integration of the Eq. (20) with respect to the azimuth angle and new variable z leads to following electron (positron) spectrum for the unpolarized case

$$\frac{d\sigma}{d\beta} = 2\alpha r_0^2\big\{A(z_0) - A(z_1) + \beta(1-\beta)\big[B(z_0) - B(z_1)\big]\big\}, \tag{22}$$

where z_0 and z_1 are the minimal and maximal values of $z\,$, $z = Arcsinh\big(\theta E/(2m)\big)$ and functions $A(z)$ and $B(z)$ are defined as follows

$$A(z) = 2z\coth z - 2\ln(2\sinh z)\ , \tag{23}$$

$$B(z) = \frac{2}{3\sinh^2 z} - 2z\coth z - \frac{2}{3}z\coth^3 z + \frac{8}{3}\ln(2\sinh z).$$

When writing the last formulae we fixed the integration constant in such a way to both $A(z),\ B(z) \to 0$ if $z \to \infty$. This choice specified by the behavior of the cross-section (16) at large $\mathbf{q}^2/m^2$.

The total cross-section in such experimental setup can be derived by elementary integration over the positron energy fraction

$$\sigma = 2\alpha r_0^2\big[\,C(z_0) - C(z_1)\big],\ C(z) = A(z) + \frac{1}{6}B(z)\ . \tag{24}$$

Note, that in the e^+e^- pair production by the photon on the stationary target with arbitrary mass M the quantity $\mathbf{q^2}$ is connected with the target mass M and the energy W of the recoil particle in the lab. system

$$\mathbf{q^2} = 2M(W - M)\,,\ \ W = \sqrt{M^2 + l^2}\,,$$

where l is the absolute value of the recoil momentum. It means that in the case of the atomic electron target $l = m\sinh(2z)\,, (M = m)$, and for the very heavy target $l = 2m\sinh(z), (M >> m)$. For the stationary target it is possible to investigate such experimental setup when detector records all events with $l > l_0\,,\ l_0 \sim m$. In this case we can formally suppose the upper limit of integration in Eq. (16) to be equal to infinity. To write the corresponding results it is enough eliminate $A(z_1), B(z_1)$ and $C(z_1)$ in Eqs. (22) and (24).

On the other hand, one can study the angular distribution of the recoil electrons. It is easy to see that in this case the angle ϑ between the photon 3-momentum and the recoil electron one $\mathbf{p_1}$ is defined by relation [2]

$$\sin^2\vartheta = \frac{4m^2}{4m^2 + \mathbf{q^2}}.$$

It means that large $\mathbf{q^2}$ correspond to small recoil angles ϑ and vice-versa. In this case $\sinh z = \cot\vartheta$.

Let us consider situation when the recoil electron is not detected. In this case we must integrate over all possible region of variation of the variable $\mathbf{q}^2$, beginning from zero. At very small $\mathbf{q}^2$, such that

$$0 < \mathbf{q}^2 < \sigma\,,\ m^6/s^2 \ll \sigma \ll m^2\,, \tag{25}$$

the differential cross section could be modified by substitution in the denominator in the r.h.s. of Eq.(19) (in accordance with definition of the cross section (3) and relation (18) for quantity q^2)

$$\mathbf{q}^4 \to \Big(\mathbf{q}^2 + \frac{m^2 s_1^2}{s^2}\Big)^2\,,\ s_1 = \frac{\mathbf{k}^2 + m^2}{\beta(1-\beta)}\,,$$

where quantity s_1 is the invariant mass squared of the created electron-positron pair in the process (1) at $\mathbf{q} = 0$. Besides, in the numerator we can neglect terms of the order of $\mathbf{q}^n$ if the power $n > 2$. In the region $\sigma < \mathbf{q}^2 < \infty$ we can use expression (19).

In the region (25) the gauge invariance requires $\mathbf{q}^2$ - dependence of the cross section of the following form [16]

$$\frac{\mathbf{q}^2}{\big(\mathbf{q}^2 + m^2 s_1^2/s^2\big)^2}\,.$$

Thus, we can perform elementary integration over $d^2\mathbf{q}$ in this region and the azimuth angle of the two-dimensional vector $\mathbf{k}$ and derive

$$\frac{d\sigma^s}{d\beta d\mathbf{k}^2} = \frac{2\alpha^3}{(m^2+\mathbf{k}^2)^2}\Big[1 - 2\beta(1-\beta) + \frac{4\beta(1-\beta)m^2\mathbf{k}^2}{(m^2+\mathbf{k}^2)^2}\Big]\Big[\ln\Big(\frac{\sigma s^2\beta^2(1-\beta)^2}{m^2(m^2+\mathbf{k}^2)^2}\Big) - 1\Big]. \tag{26}$$

To obtain the electron (positron) spectrum in the region (25) we have to integrate Eq. (26) over $d\mathbf{k}^2$. The result reads

$$\frac{d\sigma^s}{d\beta} = 2\alpha r_0^2\Big\{\big[1-\frac{4}{3}\beta(1-\beta)\big]\Big[\ln\Big(\frac{\sigma s^2\beta^2(1-\beta)^2}{m^6}\Big)-1\Big]-2+\frac{26}{9}\beta(1-\beta)\Big\}. \tag{27}$$

The total electron (positron) spectrum contains also contribution of the region $\sigma < \mathbf{q}^2 < \infty$. To derive it we integrate Eq. (20) over $\mathbf{q}^2$ and obtain

$$\frac{d\sigma^l}{d\beta} = 2\alpha r_0^2\Big[2-\ln\frac{\sigma}{m^2}+2\beta(1-\beta)\Big(\frac{2}{3}\ln\frac{\sigma}{m^2}-\frac{13}{9}\Big)\Big]. \tag{28}$$

The electron spectrum in the case of the undetected recoil electron is the sum of $d\sigma^s/d\beta$ and $d\sigma^l/d\beta$ which is defined by the well known expression

$$\frac{d\sigma}{d\beta} = 2\alpha r_0^2\big[1-\frac{4}{3}\beta(1-\beta)\big]\Big[\ln\Big(\frac{s^2\beta^2(1-\beta)^2}{m^4}\Big)-1\Big]. \tag{29}$$

It describes the corresponding differential cross section for e^+e^- pair production by the high energy photon on elementary electric charge. It is suitable also for pair production in the non-screening Coulomb field (with substitution $\alpha^3 \to \alpha^3 Z^2$.)

If the recoil electron is not detected we can also study the double distribution of the positron over the energy $\omega\beta$ and perpendicular momentum $\mathbf{k}$ which are related with its scattering angle θ : $\theta = 2|\mathbf{k}|/(\beta\sqrt{s})$. For this goal we have to integrate differential cross section (19) over $d^2\mathbf{q}$ in the region $\mathbf{q}^2 > \sigma$ and result add to contribution (26) from the region $\mathbf{q}^2 < \sigma$. Such integration of the expression (19) gives

$$\frac{d\sigma^l}{d\beta d\mathbf{k}^2} = \frac{2\alpha^3}{(m^2+\mathbf{k}^2)^2}\Big\{2\beta(1-\beta)\Big[1-\frac{6m^2\mathbf{k}^2}{(m^2+\mathbf{k}^2)^2}\Big]- \tag{30}$$
$$\Big[1-2\beta(1-\beta)+\frac{4\beta(1-\beta)m^2\mathbf{k}^2}{(m^2+\mathbf{k}^2)^2}\Big]\ln\frac{\sigma m^2}{(m^2+\mathbf{k}^2)^2}\Big\}.$$

In the total distribution the term $\ln\big(\sigma m^2/(m^2+\mathbf{k}^2)^2\big)$ cancels and we obtain

$$\frac{d\sigma}{d\beta d\mathbf{k}^2} = \frac{2\alpha^3}{(m^2+\mathbf{k}^2)^2}\Big\{2\beta(1-\beta)\Big(1-\frac{6m^2\mathbf{k}^2}{(m^2+\mathbf{k}^2)^2}\Big)+ \tag{31}$$
$$\Big[1-2\beta(1-\beta)+\frac{4m^2\mathbf{k}^2\beta(1-\beta)}{(m^2+\mathbf{k}^2)^2}\Big]\Big(2\ln\frac{s\beta(1-\beta)}{m^2}-1\Big)\Big\}.$$

When integrating (31) with respect to $d\mathbf{k}^2$, the first term in the curly brackets vanishes and we come to the spectrum (29). On the other hand we can also integrate (31) over β and obtain

$$\frac{d\sigma}{d\mathbf{k}^2} = \frac{2\alpha^3}{3(m^2+\mathbf{k}^2)^2}\Big[4\Big(1+\frac{m^2\mathbf{k}^2}{(m^2+\mathbf{k}^2)^2}\Big)\ln\frac{s}{m^2}-\frac{29}{3}-\frac{44\,m^2\mathbf{k}^2}{3(m^2+\mathbf{k}^2)^2}\Big]. \tag{32}$$

4. POLARIZATION OF THE CREATED ELECTRON

The created (fast) electron polarization in the process (1) depends on all kinematical variables and at high energies can be written as follows

$$P(\beta, \mathbf{k}, \mathbf{q}) = m\xi_2 \frac{T_{(\mu\nu)[\lambda\rho]}(e_{1\lambda}e_{2\rho} - e_{1\rho}e_{2\lambda}) 4\, p_\mu p_\nu d\Phi/q^4}{T_{(\mu\nu)(\lambda\rho)}(e_{1\lambda}e_{1\rho} + e_{2\lambda}e_{2\rho}) 4\, p_\mu p_\nu d\Phi/q^4}\,. \tag{33}$$

Note that in this equation we can eliminate factor $d\Phi/q^4$, but if our aim is, for example, to obtain the quantities $P(\beta, \mathbf{q})$ or $P(\beta)$ and so on, we first have to integrate both numerator and denominator over corresponding variables and only then to take their ratio. It is obvious that denominator is defined by the cross section and we have to investigate the numerator (or the part of the cross section which depends on circular polarization of the photon and longitudinal polarization of the created electron) in different experimental setups.

In terms of used invariants the numerator in Eq. (33) reads (without the factor $d\Phi/q^4$)

$$16m\xi_2 \Big\{ \Big[\frac{(k_2p)}{\chi_1} - \frac{(k_1p)}{\chi_2} \Big] \Big[\frac{\chi_1 + \chi_2}{\chi_1\chi_2} \big[(k_2p)(kS) + \chi_1(pS) \big] - \frac{(kp)(k_2S)}{\chi_2} \Big] + \frac{q^2(\chi_2 - \chi_1)(kp)(pS)}{2\chi_1\chi_2^2} \Big\}. \tag{34}$$

Further we use the covariant form of the electron polarization 4-vector, namely

$$S = \frac{(kk_1)k_1 - m^2 k}{m(kk_1)}. \tag{35}$$

It means that in the rest frame of the created electron $S = (0, -\mathbf{n})$, where $\mathbf{n}$ is the unit vector along the photon 3-momentum.

The used invariants are expressed through Sudakov's variables

$$2m(pS) = s\big[1 - \beta - m^2/\chi_1\big],$$

$$m(kS) = \chi_1, \quad m(k_2S) = (k_1k_2) - m^2\chi_2/\chi_1,$$

and expression into the circle braces in the r.h.s. of Eq. (34) has become very simple

$$\frac{s^2q^2}{8\chi_2}\Big[\frac{1-2\beta}{\chi_1} - \frac{m^2}{\chi_1}\Big(\frac{1}{\chi_1} - \frac{1}{\chi_2}\Big)\Big].$$

Now we can write the polarization dependent part of the cross section

$$\frac{d\sigma_\xi}{d\beta d^2\mathbf{k} d^2\mathbf{q}} = -\frac{2\alpha^3\xi_2\mathbf{q}^2}{\pi^2 q^4 (m^2 + \mathbf{k}^2)[m^2 + (\mathbf{k}+\mathbf{q})^2]}\Big[1 - 2\beta - \tag{36}$$

$$2m^2\Big(\frac{1-\beta}{[m^2+(\mathbf{k}+\mathbf{q})^2]}-\frac{\beta}{(m^2+\mathbf{k}^2)}\Big)\Big],$$

where we have to take, as before for unpolarized case, $q^4=\mathbf{q}^4$ in the region $\mathbf{q}^2>\sigma$ and $[q^2=\mathbf{q}^4+m^2s_1^2/s^2]^2$ in the region $\mathbf{q}^2<\sigma$.

For events with detected the scattered (or recoil) electron we can integrate over $d\mathbf{k}^2$ and obtain the part of the double differential cross-section in the following simple form

$$\frac{d\sigma_\xi^l}{d\beta d^2\mathbf{q}}=\frac{4\alpha^3\xi_2(1-2\beta)}{\pi\mathbf{q}^4x^2}\big[\Psi_2-\Psi_1\big]. \tag{37}$$

Note firstly that this distribution is antisymmetrical with respect to change β by $1-\beta$, whereas the polarization independent part of the cross section (see Eq. (20)) is symmetrical. Besides, at very small values of $\mathbf{q}^2$ the cross section (37) does not depend on $\mathbf{q}^2$ due to the factor x^2 in denominator whereas the cross section (20) has a pole at $\mathbf{q}^2\to 0$. The last feature implies that the polarization dependent part of the spectrum in the region $\mathbf{q}^2<\sigma$ could not have terms which contain large logarithm $\ln(s/m^2)$ that arises in the case of the pole-like behavior at $\mathbf{q}^2\to 0$.

The created electron polarization along the direction $-\mathbf{n}$, in its rest frame, is defined by the relation

$$P=\xi_2\,P(\beta,\mathbf{q}^2)=d\sigma_\xi^l/d\sigma^l,$$

so that the polarization transfer coefficient

$$P(\beta,\mathbf{q}^2)=\frac{(1-2\beta)\big(\Psi_2-\Psi_1\big)}{x^2\big[(1-2\beta(1-\beta))\Psi_1+2\beta(1-\beta)\Psi_2\big]}. \tag{38}$$

The quantity $P(\beta,\mathbf{q}^2)$ is antisymmetric relative to change $\beta\to 1-\beta$, and its magnitude is of the order unit inside a wide region of the kinematic variables. This circumstance allows to measure even a rather small values of circular polarizations.

If the scattered electrons are recorded by narrow circular detector we have to integrate over the detector aperture as described above for the unpolarized case. This procedure results

$$P(\beta)=\frac{(1-2\beta)\big[D(z_0)-D(z_1)\big]}{A(z_0)-A(z_1)+\beta(1-\beta)\big[B(z_0)-B(z_1)\big]},$$
$$D(z)=2z[tanh(z)-coth(2z)]. \tag{39}$$

If all recoil momenta with $l>l_0$ are recorded then polarization $P(\beta)$ can be derived with the same rules as it is described at the end of Sec. 3, namely one has to eliminate $A(z_1),B(z_1)$

and $D(z_1)$ in Eq. (39) and use $l_0 = 2m\sinh(z_0)$. If the angular distribution of the recoil electron is measured then one has to use $\sinh z = \cot\vartheta$.

Consider now experimental setup without detection of the scattered (or recoil) electron. Our goal is to obtain the double distribution of the created electron polarization $P(\beta, \mathbf{k}^2)$ and the spectrum-like one $P(\beta)$ by analogy with Eqs. (38) and (39). Besides we can also investigate the corresponding distribution over variable $\mathbf{k}^2$. In these cases we must take into account the contributions of both regions $\mathbf{q}^2 > \sigma$ and $\mathbf{q}^2 < \sigma$.

Integration of the r.h.s of Eq. (36) with respect to $d^{\,2}\mathbf{q}$ over the region $\mathbf{q}^2 > \sigma$ and the azimuth angle of the vector $\mathbf{k}$ gives

$$\frac{d\sigma^l_\xi}{d\beta d\mathbf{k}^2} = \frac{2\alpha^3\xi_2(\mathbf{k}^2 - m^2)}{(m^2+\mathbf{k}^2)^3}\Big[\ln\Big(\frac{\sigma m^2}{(m^2+\mathbf{k}^2)^2}\Big)\big(1-2\beta\big) + 2(1-\beta)\Big]. \tag{40}$$

We see that this part of the cross section has not a definite symmetry relative the change $\beta \to (1-\beta)$. The corresponding contribution of the region $\mathbf{q}^2 < \sigma$ is

$$\frac{d\sigma^s_\xi}{d\beta d\mathbf{k}^2} = \frac{2\alpha^3\xi_2(\mathbf{k}^2 - m^2)(1-2\beta)}{(m^2+\mathbf{k}^2)^3}\Big[1 - \ln\Big(\frac{\sigma s^2\beta^2(1-\beta)^2}{m^2(m^2+\mathbf{k}^2)^2}\Big)\Big]. \tag{41}$$

In the sum of (40) and (41) the auxiliary parameter σ cancels in the same manner as it takes place for unpolarized part of the cross section and we have

$$\frac{d\sigma_\xi}{d\beta d\mathbf{k}^2} = \frac{2\alpha^3\xi_2(\mathbf{k}^2 - m^2)}{(m^2+\mathbf{k}^2)^3}\Big\{\Big[1 - 2\ln\Big(\frac{s\beta(1-\beta)}{m^2}\Big)\Big]\big(1-2\beta\big) + 2(1-\beta)\Big\}. \tag{42}$$

Now we can write down the total distributions over β and over $\mathbf{k}^2$. The elementary integrations give

$$\frac{d\sigma_\xi}{d\beta} = 0\,,\ \frac{d\sigma_\xi}{d\mathbf{k}^2} = \frac{2\alpha^3\xi_2(\mathbf{k}^2 - m^2)}{(m^2+\mathbf{k}^2)^3}\,. \tag{43}$$

Having different distributions for both, polarization dependent and polarization independent parts of the cross section we can define the respective polarizations of the created electron $P(\beta)\,,\ P(\mathbf{k}^2)$ and $P(\beta, \mathbf{k}^2)$ by taking the corresponding ratios. Note firstly that $P(\beta)$ go to zero because $d\sigma_\xi/d\beta = 0$. Polarization $P(\mathbf{k}^2)$, that is ratio of the right hand sides of Eqs. (43) and (32) without factor ξ_2, decreases logarithmically with the rise of the photon energy because $d\sigma_\xi/d\mathbf{k}^2$ does not contain logarithmic contribution. Polarization $P(\beta\,, \mathbf{k^2})$ (the ratio of the right hand sides of Eqs. (42) and (31)) at very high energies goes to limit which does not depend on the energy

$$P(\beta\,, \mathbf{k^2})|_{s\to\infty} = \frac{(m^4 - \mathbf{k}^4)(1-2\beta)}{(m^2+\mathbf{k}^2)^2 - 2\beta(1-\beta)(m^4+\mathbf{k}^4)}\,. \tag{44}$$

The quantity $P(\beta)$ vanishes (with the accuracy of m/ω) if we take into account all events with $0 < \mathbf{k}^2 < \infty$. But the elimination the region of the very small values of $\mathbf{k}^2$ increases (in absolute value) the events number which depends on the photon circular polarization and decreases the unpolarized events number. Therefore, the created electron polarization can be determined with high efficiency by the spectrum distribution of the created electron (or positron) using the following constraint on the event selection

$$\mathbf{k}^2 > \mathbf{k}_0^2 \,,$$

where $\mathbf{k}_0^2$ is of the order of a few m^2. The above restriction means that events with very small angles of the created electron and positron are excluded.

The simple calculation gives for the electron polarization in such experimental setup

$$P(\beta, \mathbf{k}_0^2) = \frac{y(1+y)A(s,\beta)}{B(y,s,\beta)} \,,\ y = \frac{\mathbf{k}_0^2}{m^2} \,, \tag{45}$$

where

$$A(s,\beta) = 2(1-\beta) + \Big[1 - 2\ln\Big(\frac{s\beta(1-\beta)}{m^2}\Big)\Big]\big(1-2\beta\big) \,,$$

$$B(y,s,\beta) = \Big[(1+y)^2 - \frac{2}{3}\beta(1-\beta)(2+3y+3y^2)\Big]2\ln\Big(\frac{s\beta(1-\beta)}{m^2}\Big) -$$

$$-(1+y)^2 + \frac{4}{3}\beta(1-\beta)(1+3y^2) \,.$$

5. NUMERICAL RESULTS AND DISCUSSIONS

In this section we demonstrate some numerical estimates for the created electron polarization (along the photon 3-momentum direction in its rest frame) for different experimental situations. Together with polarizations we show the corresponding unpolarized parts of the cross section for which we always use units $[\mu b]$ or $[\mu b/MeV^2]$. The results for different experimental setups with detection of the recoil (or scattered) electron are shown in Figs. 3–6 and without detection – in Figs. 7,8. All curves in these figures are correct when the condition $s >> \mathbf{q^2}, \mathbf{k^2}, m^2$ is satisfied, and we suggest that the minimal value of the recoil 3-momentum always is of the order of m. In this case different unpolarized differential cross sections are symmetric with respect to change $\beta \to (1-\beta)$ whereas the polarizations are antisymmetric.

Note that all curves in Figs. 3,5,6 do not depend on the collision energy (only the above mentioned constraints on values $s, \mathbf{q}^2$ and m^2 are suggested correct), and the curves in Fig. 4

depend. The reason is that in Fig. 4 we give the corresponding distributions for events in c.m.s. with the fixed scattered electron angles (but not $\mathbf{q}^2$). Inside the used accuracy these angles are expressed via the perpendicular momentum transferred and the initial electron energy by simple relation $\mathbf{q}^2 = \theta^2\, E^2,\ E = \sqrt{s}/2$. It means that at fixed θ the value of $\mathbf{q}^2$ increases as the second power of the energy but, as it follows from Fig. 3, the cross section decreases very quickly with the growth of $\mathbf{q}^2$.

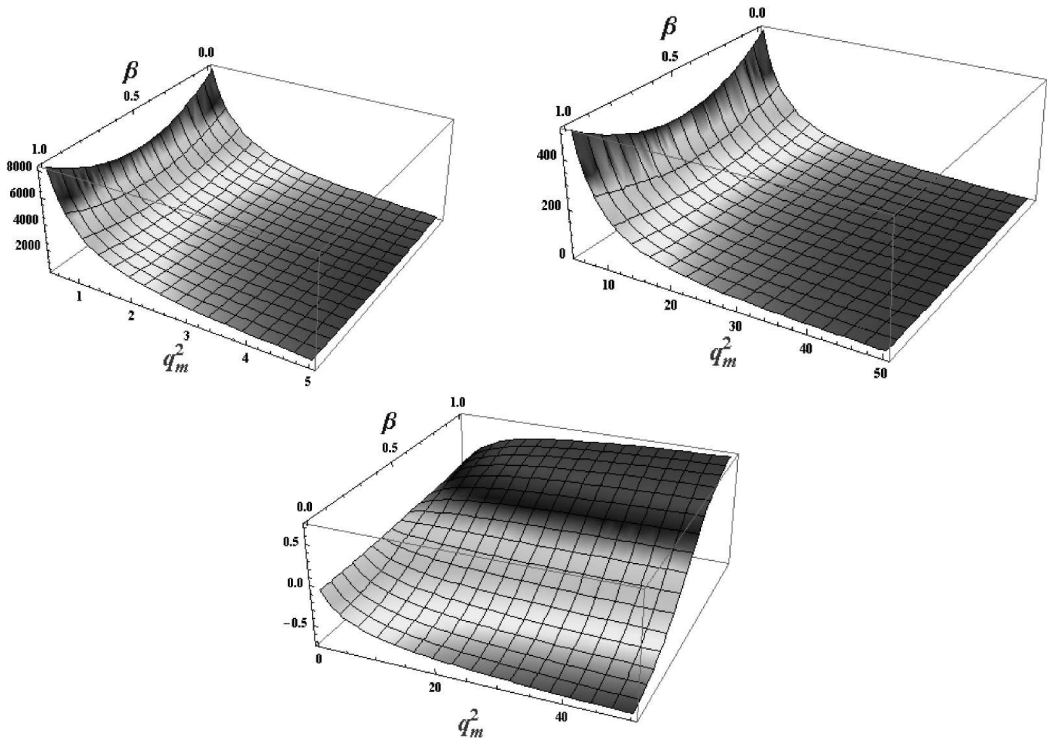

Fig.3. *Double differential cross section (two upper graphs) as defined by Eq.(20) and the respective distribution for the electron polarization given by Eq.(38). The energy fraction of the electron is* $\omega(1-\beta)$ *and* $q_m^2 = \mathbf{q}^2/m^2$.

To imagine the energy dependence of the curves in Fig. 4 we perform corresponding calculations also at $E = 1\,GeV$ and $10\,GeV$ and can to say that polarization practically do not depend on the energy whereas the cross section lost more then three orders when the energy goes from $100 MeV$ to $10\,GeV$.

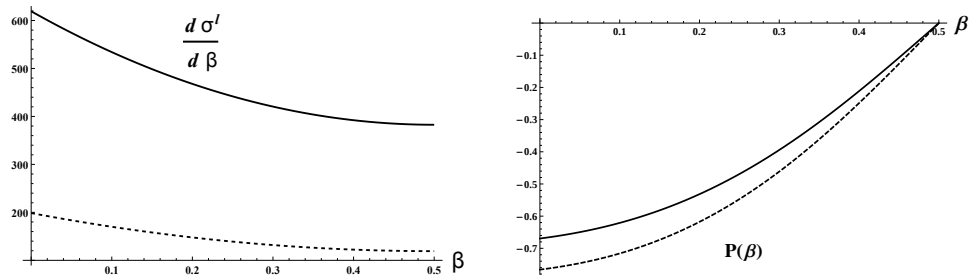

Fig.4. *The unpolarized part of the cross section and polarization of the created electron given by Eqs. (22) and (39) in the reaction c.m.s. (with* $z_0 = Arcsinh(\theta_{min}E/2m)$ *and* $z_1 = Arcsinh(\theta_{max}E/2m)$*) at* $E = 100\,MeV$ *for events with minimal electron scattering angles* $\theta_{min} = 1^o$ *(solid curves),* $\theta_{min} = 2^o$ *(dotted curves) and* $\theta_{max} = 6^o$ *in both cases.*

There is absolutely different picture of the angular distribution of the recoil electrons for events in the rest frame. In this case the relation between the scattered angle and the perpendicular momentum transferred does not contain collision energy. Therefore the curves in Fig.5 are the same at above mentioned energies. Because in the rest frame

$$\mathbf{q}^2 = 4m^2cot^2(\vartheta)$$

the cross section decreases with the growth of the recoil electron scattering angle θ.

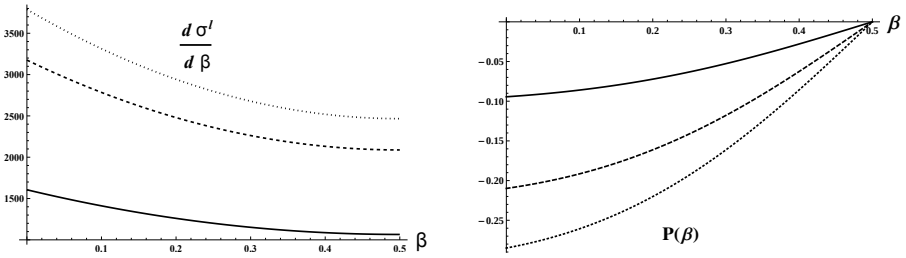

Fig.5. *The same quantities as in Fig. 4 but for events in the rest frame of the initial electron with* $z_0 = Arcsinh[\cot(\vartheta_{max})]$ *and* $z_1 = Arcsinh[\cot(\vartheta_{min})]$ *in Eqs. (22) and (39). We use* $\vartheta_{max} = 75^o$ *and* $\vartheta_{min} = 60^o$ *(solid lines),* $\theta_{min} = 30^o$ *(dashed lines),* $\vartheta_{min} = 5^o$ *(dotted lines).*

To be complete with description of events at recorded the scattered (or recoil) electron we also give in Fig. 6 the unpolarized cross section and polarization at different values of the minimal magnitude of the recoil electron 3-momentum.

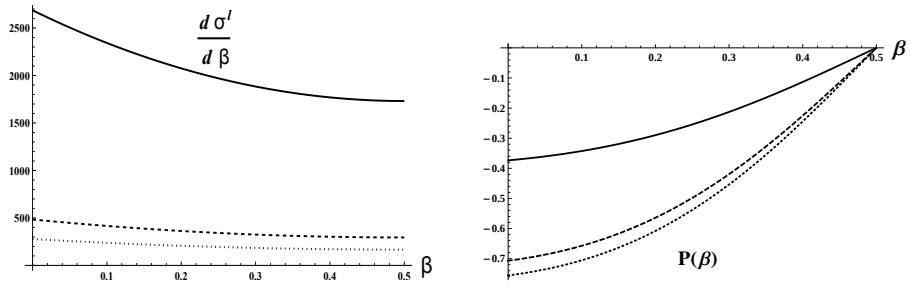

Fig.6. *The same quantities as in Fig. 5 but at* $z_0 = Arcsinh(l_0/m)/2$ *and* $A(z_1) = B(z_1) = D(z_1) = 0$ *in Eqs. (22) and (39);* $l_0 = m$ *(solid curves),* $l_0 = 10\,m$ *(dashed curves), and* $l_0 = 20\,m$ *(dotted curves).*

As concern the experimental setup without detection of the recoil (or scattered) electron, the corresponding events include, by definition, all values of $\mathbf{q}^2$ from zero ones. In this case, the dependence of the differential cross section $d\sigma/d\beta d^2\mathbf{k}d^2\mathbf{q}$ on the collision energy arises due to $1/q^4$ factor in Eq. (3). After integration of the cross section relative $d^2\mathbf{q}$ this dependence leaves a trace as a term enhanced by the logarithmic factor in Eq. (31). They say that such integrated cross section increases logarithmically with growth of the energy.

In Fig. 8 we show the differential cross section and polarization of the electron as a function of the positron perpendicular momentum only. As we pointed out above, the cross section increases logarithmically with the energy whereas the polarization decreases. In spite of this circumstance the polarization can be measured using such kind of distribution up to energies $s = 1GeV^2$, because the corresponding event number is large enough. The more advantageous situation takes place when events with $0 < \mathbf{k}^2 < \mathbf{k}_0^2$ are excluded and then the polarization increases with the collision energy (it is demonstrated in Fig. 9). The unpolarized cross section in this figure is not given in text, but can be derived by integration of the cross section (31) with respect to $\mathbf{k}^2$ from $\mathbf{k}_0^2$ up to ∞.

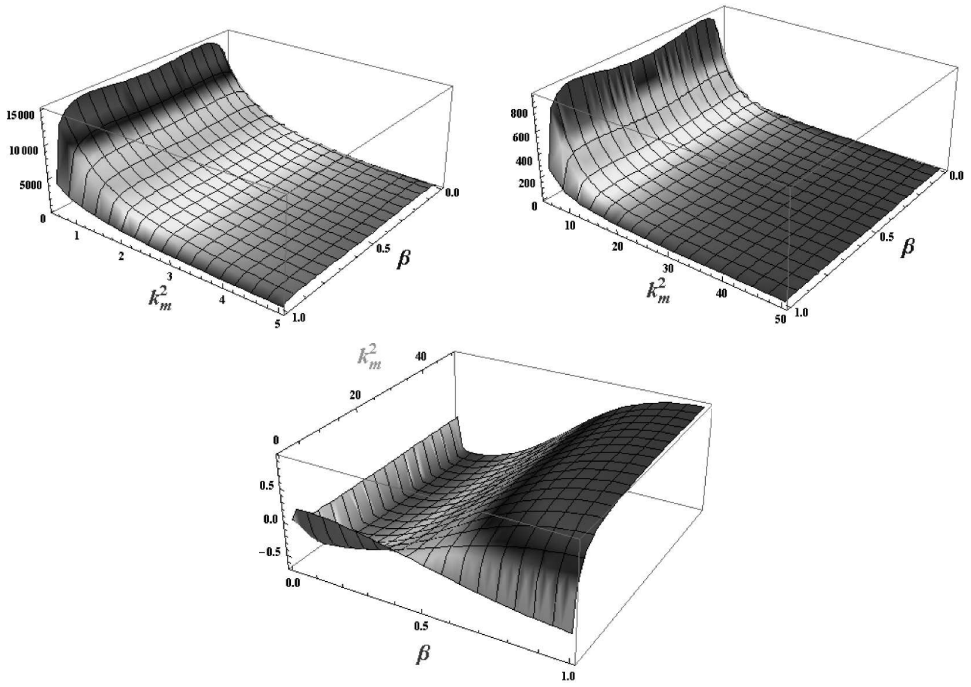

Fig.7. *Double differential cross section (two upper figures) as defined by Eq. (31) and the respective distribution for the electron polarization, that is the ratio of the right hand side of Eq. (42) at* $\xi_2 = 1$ *to the cross section (31), at* $s = 300\,MeV^2$, $k_m^2 = \mathbf{k}^2/m^2$.

Let us compare our developed approach and obtained results with the corresponding investigations in Ref. [14]. Note first that in both papers only the Borselino diagrams have been taken into account for theoretical description of the process (1) and the Sudakov's variables have been used. In Ref. [14] the polarization of both components of the created pair is considered but we concentrated on the polarization of the fast electron only. In Ref. [14] the calculations were performed in the leading logarithmic approximation using the equivalent photon method whereas our results include also contribution which does not depend on the energy. We consider different event selections, particularly distributions on the recoil electron variables, which can not be studied by the method used in Ref. [14].

Thus, we must compare formula (14) in Ref. [14] with coefficient at $\ln(s/m^2)$ in our unpolarized (Eq. (26)) and polarized (Eq. (41)) cross sections caused by small values of $\mathbf{q}^2 < \sigma$. We see first that our unpolarized cross section is twice as compared with one in Ref. [14]. It means that we perform the spin summation. We also use polarized cross section

that has to be twice as compared with one in Ref. [14] (if suppose $\xi = \lambda\,,\ \delta_- = 1$). But we see that this is not so. The reason is that we take different parametrization for the electron polarization 4-vector (see Eq. (35) in our work and Eq. (12) in Ref. [14]). Let $\tilde{S}$ is the polarization 4-vector used in Ref. [14]. Then we have in our notation

$$2m(p\tilde{S}) = s(1-\beta)\,,\ m(k\tilde{S}) = \chi_1 - \frac{m^2}{1-\beta}\,,\ m(k_2\tilde{S}) = (k_1k_2) - \frac{m^2\beta}{1-\beta}\,.$$

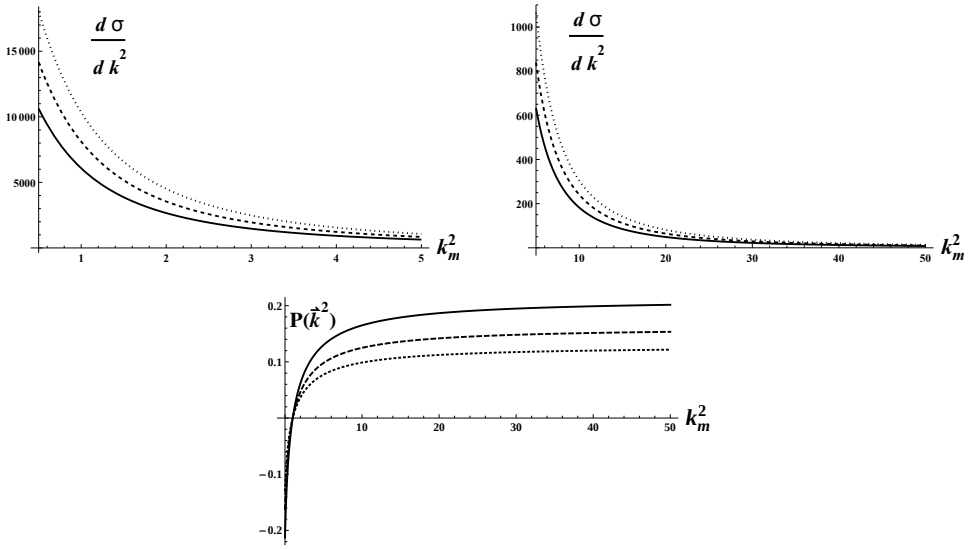

Fig.8. *Differential cross section as defined by Eq. (32) and the respective polarization, that is the ratio of the right hand side of Eq. (43) at $\xi_2 = 1$ to the cross section (32), at $s = 100\,MeV^2$ (solid curves), $s = 300\,MeV^2$ (dashed curves) and $s = 1\,GeV^2$ (dotted curves).*

These relations distinguish from the corresponding ones but with 4-vector S instead of $\tilde{S}$ (see formulas on page 15 after Eq. (35)). Just this distinction is a source of different forms of the polarization dependent parts of the differential cross sections. We take attention also that in accordance with Eq. (43) our respective spectral distribution vanishes for both contributions: leading logarithmic and constant ones, whereas in Ref. [14] the logarithmic contribution is non-zero (Eq. (16)).

Unpolarized cross section, within adopted accuracy, is symmetric relative change $\beta \rightleftarrows (1-\beta)$. With our choice of the 4-vector S the created electron polarization is antisymmetric if the recoil (or scattered) electron is recorded. Otherwise, there are non-logarithmic contributions which do not posses definite symmetry under this change (see Eqs. (42), (45)).

The accuracy of our calculations is restricted by neglected terms of the order of m^2/s and by the radiative corrections. The first ones can be essential near the boundaries of the electron spectrum [8]. Therefore our calculations are valid for the region $0.1 < \beta < 0.9$. As to the radiative corrections, they violate the above mentioned symmetries on the percent level in this region of the electron energies, at least for unpolarized events, due to possibility of the hard photon emission [19].

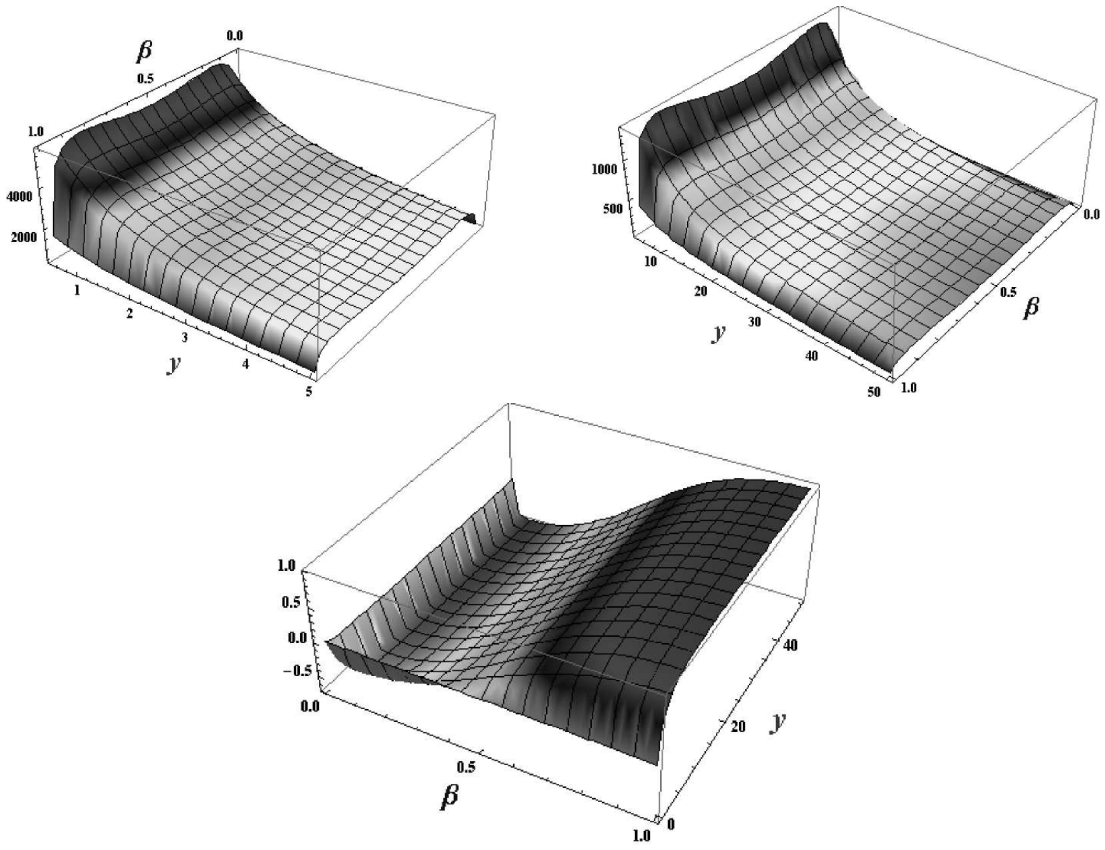

Fig.9. *Differential cross section (two upper figures) and the created electron polarization (Eq. (45)) as a function of the energy fraction β and parameter y at $s = 300\,MeV^2$.*

6. CONCLUSION

The process of the e^+e^--pair production in the scattering of the circularly polarized photon beam on the electrons leads to the origin of the polarization of the produced electron and positron. At high energy of the photon beam this effect can be used both for the production of the high-energy polarized electron (and positron) (see Ref. [14]) and for the measurement

of the photon circular polarization degree since the differential cross section and polarization transfer coefficient do not decrease with the photon energy growth. The main contribution to these physical quantities is caused by the events with small momentum transfer squared ($|q^2|/s \ll 1$) when e^+e^--pair carries away all photon energy. This contribution is determined by the Borselino diagrams (Fig. 1).

In our paper this contribution has been calculated for different distribution of the final particles using the technique of the Sudakov variables. We considered two essentially different physical situations. The first one is concerned with the detection not only produced electron but also the scattered (recoil) electron. That kind of detection is quite possible since the final electrons belong to different (non-overlapped) phase space regions. The results of our numerical calculations are presented in Figs. 3-6 for the case when minimal transverse transfer momentum is of the order of the electron mass ($|\vec{q}^{\,2}|_{min} \approx m^2$).

The typical differential cross sections turn out to be of the order of 1 mb and the polarization transfer coefficients are of the order of 1 and antisymmetrical relative the change $\beta \to (1-\beta)$. Our calculations imply the integration over total interval of the electron azimuthal angles. In principle, they can be done for any detector geometry since the differential cross section (the formulas (19) and (36)) is easy to integrate numerically.

The results of calculations in case when the scattered electron is not detected are presented in Figs. 7-9. In these calculations the contributions of all events with $|\vec{q}^{\,2}| \geq 0$ are added together. The differential cross section (formulas (31) and (42)) acquire the contribution which growth logarithmically with the energy. At the cost of this the cross sections turn out to be somewhat larger than in the first case. The polarization transfer coefficient is also of the order of 1 if the electron energy is measured but it is essentially smaller if the integration over the energy is done in all range of values (Fig. 8). It is important to note that such experimental set up is possible in the interaction of photons with the electron beam since during the interaction of the photons with a matter the scattering on the atomic electrons with the e^+e^--pair production (without recoil electron detection) will be only the background process relative the Bethe-Heitler process.

Authors thank A. Glamzdin for helpful discussion.

---

1. V.F. Boldyshev, Yu.P. Peresunko, Yad. Fiz. **14**, 1027 (1971); **19**, 144 (1974);

2. E.A.Vinokurov, E.A. Kuraev, Zh. Eksp. Theor. Fiz. **62**, 1142 (1973).
3. E.A.Vinokurov, N.P. Merenkov, Yad. Fiz. , **21**, 781 (1975).
4. V.F. Boldyshev, E.A.Vinokurov, N.P. Merenkov, Yu.P. Peresunko, Physics of Elementary Particles and Atomic Nuclei **25**, 696 (1994).
5. I. Endo, S. Kasai, M. Harada et al., Nucl. Instr. and Meth. A **280**,144 (1989).
6. E. Haug, Phys. Rev. D **31**, 2120 (1985); D **32**, 1594 (1985).
7. A. Borselino, Il Nuovo Cimento **4**, 112 (1947).
8. I.V. Akushevich, H. Anlauf, E.A. Kuraev et al.,Phys. Rev. A **61**, (2000) 032703.
9. A.S. Arichev, A.P. Potylitsin, M.N. Strikanov, arXiv:0112060[ph], 2001, 9p.
10. G.L.Kotkin, V.G. Serbo, V.I. Telnov, Phys. Rev., ST-Accel and Beams, 2003, p.011001-011006.
11. A.I. Akhiezer, V.B. Berestetsky, Quantum Electrodynamics. Moscow, Nauka 1969.
12. A.A. Abdo, M. Ackermann, M. Ajello et al., Astroph. J. **708**, 1254 (2010).
13. L. Kuiper, W. Hermsen, G. Cusumano et al., Astron. and Astroph. **378** , 918 (2001).
14. V.V. Byyev, E.A. Kuraev, M.V. Galinsky, A.P. Potylitsin, Pisma. Zh. Eksp. Teor. Fiz. **75**, 542 (2002).
15. V.A. Khoze, M.I. Konchanij, N.P. Merenkov et al., Eur. Phys. J. C **25**, 1999 (2002); H.Czyż, A.Grzelinska, J.H. Kühn and G. Rodrigo, Eur. Phys. J. C **47**, 617 (2006); A. Denig, Nucl. Phys. Proc. Suppl. **162**, 81 (2006).
16. V.V. Sudakov, Zh. Eksp. Teor. Fiz. **30**, 87 (1956); V.G. Gorshkov, Usp. Fiz. Nauk **10**, 45 (1973).
17. C. Weizsacker, Zs. f. Phys. **88**, 612 (1934); E. Williams, Phys. Rev. **45**, 729 (1934).
18. K.S. Suh and H.A. Bethe, Phys. Rev. **115**, 672 (1959).
19. E.A. Vinokurov, E.A. Kuraev, N.P. Merenkov, Zh. Eksp. Teor. Fiz. **66**, 1916 (1974).